

# Coupling Characteristics of Nonradiative Dielectric Waveguides

TSUKASA YONEYAMA, MEMBER, IEEE, NORIO TOZAWA, AND SHIGEO NISHIDA, SENIOR MEMBER, IEEE

**Abstract**—An analytical method is presented for predicting coupling characteristics of dielectric strips in the nonradiative dielectric waveguide. Starting with an approximate but very accurate expression for the coupling coefficient between parallel dielectric strips, the scattering coefficients for nonuniform coupling structures are derived in simple closed-form expressions by taking the effect of the field deformation at the curved sections into account. The coupling coefficient of the nonradiative dielectric waveguide is found to be so large compared to those of other dielectric waveguides that complete power transfer can be attained with coupled polystyrene bends having a curvature radius as small as 20 mm at 50 GHz. The theory was verified experimentally for various coupling structures.

As an application toward millimeter-wave integrated circuits, 0-dB couplers, quadrature hybrid couplers, and an in-phase power divider were constructed based on the present analysis. A comparison of theory and experimental data of these fabricated coupling circuits suggests that the effect of the nondegenerate modes in the straight and curved guides must be included in the analysis to further improve the theory.

## I. INTRODUCTION

THE DEVELOPMENT of high-performance and low-cost integrated circuits is of highest importance for the realization of the full potential of millimeter-wave systems [1]. The nonradiative dielectric waveguide (NRD-guide) has been proposed as a favorable transmission line for achieving such an objective. Though it is a dielectric waveguide resembling the *H*-guide in structure, undesirable radiation at bends and other discontinuities can be substantially suppressed by the cutoff nature of the conducting plates which are separated by less than half a wavelength. Basic characteristics of the NRD-guide are fully understood [2], and some passive components [3] and bends [4] have also been investigated experimentally. As a further step in the development of the NRD-guide technique, directional couplers will be considered in this paper. They are important in various applications including ring resonators [3], [5], channel dropping filters [6], balanced mixers [7], and others [8].

Many authors have studied coupling characteristics of millimeter-wave dielectric waveguides and pointed out that the coupling action between the connecting guides cannot be at all neglected [9], [10], [11]. Usually, this additional effect is taken into account by integrating the variable coupling coefficient along the axial direction of the coupler under the tacit assumption that the guides are moderately curved. In the NRD-guide couplers, however, very sharp bends are expected to be put to use since there is no

trouble with radiation. Therefore, the effects of the field deformation at a bend, as well as of the nonuniform coupling spacing, must be included in the analysis. Following the method of Marcuse [12], an approximate but very accurate expression for the coupling coefficient of a simple parallel NRD-guide coupler is derived first, and then modified so as to be applicable to nonparallel coupling structures consisting of circular bends of an arbitrary bending angle based on certain admissible assumptions. Thus, the scattering coefficients of the directional couplers can be obtained in simple closed-form expressions.

In the course of the analysis, the coupling coefficient of the NRD-guide is found to be larger than those of other dielectric waveguides. This fact implies that compact couplers can be realized with the NRD-guide. Indeed, complete power transfer could be attained between two identical polystyrene bends with a curvature radius as small as 20 mm at 50 GHz.

The theory was verified by measurements and applied to the fabrication of 0-dB couplers, quadrature hybrid couplers, and an in-phase power divider using polystyrene dielectric. The fabricated circuit components were tested at 50 GHz and generally confirmed to operate as expected. However, the power divider which consists of three coupled nonparallel guides [8] is too complicated in structure to be treated within the scheme of the present theory. This fact suggests that the effect of the nondegenerate modes in the straight and curved guides is substantial and must be included in the analysis. In spite of such a limitation in applicability, the coupling expressions derived here are capable of predicting the performance of the two coupled nonparallel waveguides precisely and are thus very useful for designing many coupling circuits.

## II. COUPLING COEFFICIENT OF PARALLEL COUPLER

The rigorous solution has been obtained for the coupling coefficient of a parallel NRD-guide coupler [2] but seems to be too complicated for application to nonparallel coupling structures. Instead of relying on it, another simpler expression will be derived by means of Marcuse's method [12]. The expression is approximate, but very accurate and easy to extend to nonparallel couplers.

Marcuse's coupling formula for degenerate modes in general dielectric waveguides, when simplified to homogeneous and lossless guides, reduces to

$$C = \sqrt{C_1 C_2} \quad (1)$$

Manuscript received December 16, 1982, revised April 5, 1983.

The authors are with the Research Institute of Electrical Communication, Tohoku University, Katahira 2-1-1, Sendai, 980 Japan.

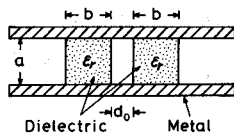


Fig. 1. Cross-sectional view of coupled dielectric strips in the nonradiative dielectric waveguide.

where

$$C_1 = \frac{\omega \epsilon_0 (\epsilon_{r1} - 1)}{4} \int_{S_1} \mathbb{E}_1^* \cdot \mathbb{E}_2 dS \quad (2a)$$

$$C_2 = \frac{\omega \epsilon_0 (\epsilon_{r2} - 1)}{4} \int_{S_2} \mathbb{E}_2^* \cdot \mathbb{E}_1 dS. \quad (2b)$$

In the above equations,  $\mathbb{E}_1$  and  $\mathbb{E}_2$  are the mode electric fields of guides 1 and 2 in isolation, respectively, and are normalized with respect to unit transmission power,  $\epsilon_{r1}$  and  $\epsilon_{r2}$  are the relative dielectric constants,  $S_1$  and  $S_2$  are the cross-sectional areas of the respective waveguides over which integration is carried out, and the asterisk indicates the complex conjugate (see [12, (26)] for more detail). The coupling coefficient  $C$  is the geometric mean of coefficients  $C_1$  and  $C_2$ . Coefficient  $C_1$  can be interpreted as being a one-way coupling coefficient from guide 2 to guide 1, while coefficient  $C_2$  has the same effect from guide 1 to guide 2. If both the waveguides are identical and carry the same mode, coefficients  $C_1$  and  $C_2$  are also identical. But, when they are different in either their structures or mode configurations,  $C_1$  and  $C_2$  are no longer the same. Such is the case when the straight and curved guides are coupled, as will be considered later.

For a simple parallel NRD-guide coupler as shown in Fig. 1, (1) and (2) yield

$$C = K \exp(-pd_0) \quad (3)$$

where

$$K = \frac{\epsilon_r p^2 q^2}{\beta \{ [q^2 + (\epsilon_r p)^2] (pb/2) + \epsilon_r (p^2 + q^2) \}} \quad (4a)$$

$$\beta = \sqrt{\beta_0^2 - (\pi/a)^2}. \quad (4b)$$

In the above equations,  $d_0$  is the coupling spacing,  $\beta_0$ ,  $q$ , and  $p$  are the propagation constant, the transverse phase constant, and the transverse decay constant, respectively, of the lowest TM surface-wave mode supported by a slab whose relative dielectric constant is  $\epsilon_r$ , and whose thickness is  $b$ , and  $\beta$  is the propagation constant of the NRD-guide whose conducting plate separation is  $a$  and whose strip width is the same as the slab thickness  $b$ .

The coupling coefficient given by (3) is identical with that for the coupled TM slab waveguides as derived by Marcuse, except that the propagation constant  $\beta$  in the denominator of (4a) is replaced by  $\beta_0$  in the latter case. This similarity may be inferred from a physical consideration of propagation mechanisms in both the dielectric waveguides. Since  $\beta$  is smaller than  $\beta_0$  due to the presence of the term  $(\pi/a)^2$  in (4b), the coupling coefficient of the NRD-guide is much larger than that of the slab waveguide, and also probably larger than those of other dielectric

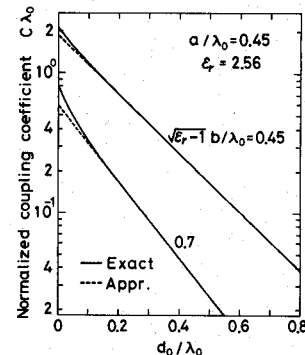


Fig. 2. Comparison of exact and approximate coupling coefficients for a parallel nonradiative dielectric waveguide coupler.

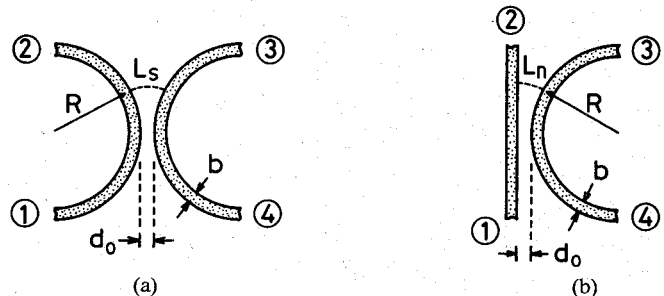


Fig. 3. Configurations of: (a) symmetric coupler; and (b) nonsymmetric coupler.

waveguides. The immediate implication of this is that substantial reduction in circuit size is possible with the NRD-guide.

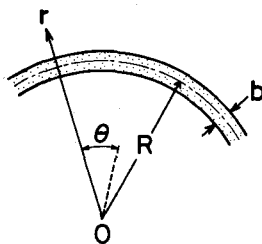
For the sake of comparison, (3) is computed and presented in Fig. 2 together with the exact values obtained previously [2]. Agreement between them is excellent, especially when the coupling spacing is not too small.

### III. COUPLING CHARACTERISTICS OF CURVED NRD-GUIDE

#### A. Preliminary Remarks

Most practical dielectric waveguide couplers have curved or angled connecting arms which are joined to the input and output terminals. Typical configurations would be symmetric and nonsymmetric couplers containing circular bends as shown in Fig. 3(a) and (b), respectively [11]. Since bends can be very sharp in the NRD-guide, the effect not only of the nonuniform coupling spacing, but also of the field deformation at a bend must be taken into account in the analysis.

In (3), factor  $K$  can be considered to be less sensitive to the field deformation than the other factor of the exponential function, because the former depends on the gross value of the field intensity integrated over the cross section of the guide, while the latter is the mode field intensity itself of one guide at the wall of the other. Therefore, expression (4a) for  $K$  can be assumed to be valid even for the curved guides as well. The exponential function in (3), however, must be replaced by a field expression appropriate to the curved guide, if the coupler consists of bends.

Fig. 4. A circular bend in cylindrical coordinates  $(r, \theta)$ .

Behavior of a bend in the NRD-guide is complicated [4], but if the curvature radius is not too small, the radial field variation in close proximity to the circularly curved dielectric strip can be approximated by [13]

$$\begin{aligned} E(r) &\sim \exp \left\{ - \int_{R+b/2}^r \left[ \left( \frac{\beta R}{r} \right)^2 + \left( \frac{\pi}{a} \right)^2 - k_0^2 \right]^{1/2} dr \right\} \\ &\simeq \exp \left( -p \left\{ \left( r - R - \frac{b}{2} \right) - \frac{\beta^2}{2p^2 R} \left[ (r - R)^2 - \left( \frac{b}{2} \right)^2 \right] \right\} \right) \end{aligned} \quad (5)$$

where  $R$  is the curvature radius of the bend and  $r$  is the radial coordinate as shown in Fig. 4. Integration in (5) is carried out by expanding the integrand into the power series in terms of the fractional distance  $(r - R)/R$  leaving only the first two terms. Since the field expression is at hand, the coupling coefficient of the curved guides can then be derived.

### B. Symmetric Coupler

In the symmetric coupler as shown in Fig. 3(a), the equiphasic fronts of the propagating modes change into cylindrical surfaces as a result of interaction between the fields in the two curved guides; hence the coupling spacing is given by the arclength  $L_s$  between the incremental coupling lengths of both the guides [11]. Equating  $(r - R - b/2)$  with  $L_s$  in (5) and substituting the resulting equation for the exponential function in (3) gives the following expression for the coupling coefficient of the two circular bends:

$$C = K \exp \left\{ -p L_s \left[ 1 - \frac{\beta^2}{2p^2 R} (L_s + b) \right] \right\}. \quad (6)$$

On the other hand, the arclength is written as

$$L_s = \frac{d_0 + 2(R + b/2)(1 - \cos \theta)}{\sin \theta} \theta \quad (7)$$

where  $\theta$  is the angular coordinate. The scattering coefficients of the directional coupler could be obtained by substituting (7) into (6) and integrating the resulting equation numerically with respect to  $\theta$  [11]. But, a simpler method would be to approximate (7) as

$$L_s \simeq d_0 + \left( R + \frac{b}{2} \right) \theta^2 \quad (8)$$

under the assumption that coupling is effective only for small values of  $\theta$ . Substituting (8) into (6) and integrating the resulting equation with respect to  $\theta$  from negative to positive infinity leads to the following closed-form expres-

sions for the scattering coefficients of the symmetric directional coupler:

$$|S_{21}| = |\cos(C_s l_s)| \quad (9a)$$

$$|S_{31}| = |\sin(C_s l_s)| \quad (9b)$$

where

$$C_s = K \exp \left\{ -p d_0 \left[ 1 - \frac{\beta^2}{2p^2 R} (d_0 + b) \right] \right\} \quad (10a)$$

$$l_s = R \left\{ \frac{\pi}{p \left( R + \frac{b}{2} \right) \left[ 1 - \frac{\beta^2}{p^2 R} \left( d_0 + \frac{b}{2} \right) \right]} \right\}^{1/2}. \quad (10b)$$

Coefficient  $C_s$  is the coupling coefficient at the minimum coupling spacing ( $\theta = 0$ ), and  $l_s$  is the effective coupling length. It should be noted that the above equations are valid for any symmetric couplers having arbitrary, but not too small, bending angles. This is obvious, since coupling is negligible beyond some value of  $\theta$  smaller than the bending angles of common coupling structures.

If the field deformation at a bend is ignored, the expressions for  $C_s$  and  $l_s$  reduce to

$$C_s = K \exp(-p d_0) \quad (11a)$$

$$l_s = R \left\{ \frac{\pi}{p \left( R + \frac{b}{2} \right)} \right\}^{1/2}. \quad (11b)$$

Comparison of (10) and (11) clearly shows that the field deformation acts to increase both quantities  $C_s$  and  $l_s$ . The reason for this is that the field raises its intensity in the outer side of the bend [4].

### C. Nonsymmetric Coupler

A similar argument holds for nonsymmetric couplers as well. In this case, however, coefficients  $C_1$  and  $C_2$  are no longer the same because of the nonsymmetric structure. The effect of the field deformation is included only in coefficient  $C_1$  but not in  $C_2$ . The coupling coefficient for a straight guide applies to  $C_2$  since the one way coupling comes from the straight guide. If the separation along the arc between the incremental coupling lengths of the guides is denoted by  $L_n$ , coefficients  $C_1$  and  $C_2$  can be expressed as

$$C_1 = K \exp \left\{ -p L_n \left[ 1 - \frac{\beta^2}{2p^2 R} (L_n + b) \right] \right\} \quad (12a)$$

$$C_2 = K \exp(-p L_n). \quad (12b)$$

Hence, the coupling coefficient  $C$  is given by

$$C = K \exp \left\{ -p L_n \left[ 1 - \frac{\beta^2}{4p^2 R} (L_n + b) \right] \right\}. \quad (13)$$

Since the arclength  $L_n$  can be approximated as

$$L_n \simeq d_0 + \frac{1}{2} \left( R + \frac{b}{2} \right) \theta^2 \quad (14)$$

substituting (14) into (13) and integrating the resulting

equation with respect to  $\theta$  from negative to positive infinity results in

$$|S_{21}| = |\cos(C_n l_n)| \quad (15a)$$

$$|S_{31}| = |\sin(C_n l_n)| \quad (15b)$$

where

$$C_n = K \exp \left\{ -p d_0 \left[ 1 - \frac{\beta^2}{4p^2 R} (d_0 + b) \right] \right\} \quad (16a)$$

$$l_n = R \left\{ \frac{2\pi}{p \left( R + \frac{b}{2} \right) \left[ 1 - \frac{\beta^2}{2p^2 R} \left( d_0 + \frac{b}{2} \right) \right]} \right\}^{1/2} \quad (16b)$$

Most comments regarding a symmetric coupler are equally valid for a nonsymmetric coupler. Furthermore, comparing (10b) and (16b) shows that the effective coupling length of a nonsymmetric coupler is larger than that of a symmetric coupler by a factor of about  $\sqrt{2}$ . This is to be expected because the coupling spacing of a nonsymmetric coupler varies more slowly as a function of the angular coordinate  $\theta$ .

If the effect of the field deformation is ignored, (16a) and (16b) reduce to

$$C_n = K \exp(-pd_0) \quad (17a)$$

$$l_n = R \left[ \frac{2\pi}{p \left( R + \frac{b}{2} \right)} \right]^{1/2} \quad (17b)$$

#### IV. MEASUREMENTS

##### A. Verification of Theory

In order to confirm the theory, frequency dependence of coupling  $|S_{31}|$  was measured at 50 GHz. Dielectric strips, 2.7 mm in thickness and 2.4 mm in width, were made of polystyrene with a relative dielectric constant of 2.56. Measurements were made for both the symmetric and nonsymmetric couplers. Two types of symmetric couplers were fabricated, one consisting of 180° bends with a curvature radius of 20 mm and the other consisting of 90° bends with a curvature radius of 65 mm. The nonsymmetric coupler was constructed by coupling a straight guide and a 180° bend with a curvature radius of 20 mm. A photograph of them is shown in Fig. 5.

A 20-mm curvature radius was chosen since no appreciable reflection takes place at a bend if the curvature radius is not smaller than 20 mm [4]. In order to minimize the effect of the transmission loss of about 13 dB/m in measurements, the substitution method was used with a straight guide equal in length to the bends as the standard of comparison. Matched terminations, if necessary, were provided by attaching thin resistive absorbers on the surfaces of the dielectric strips [3].

Theoretical and measured data of  $|S_{31}|$  are compared in Fig. 6(a), (b), and (c). Solid curves are calculated by taking the field deformation into account, while dotted curves are

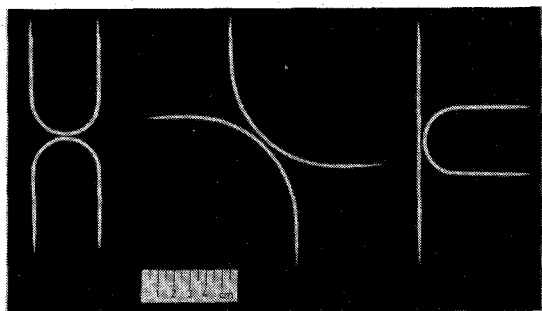
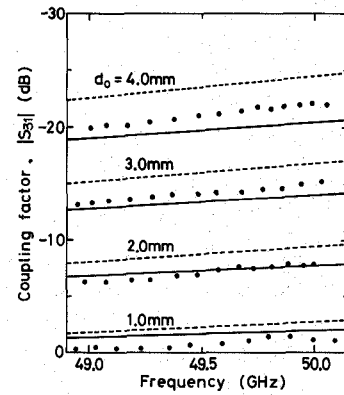
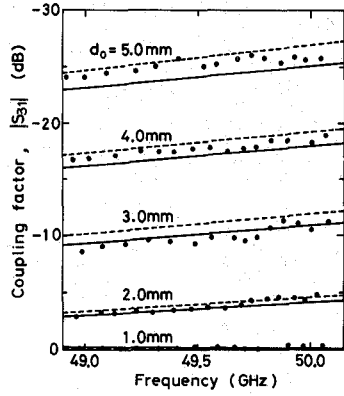


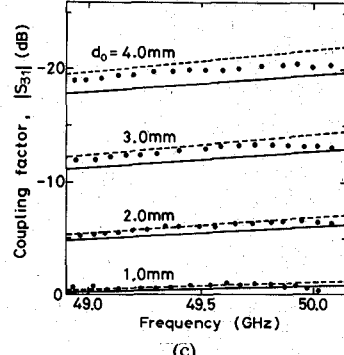
Fig. 5. Photograph of fabricated directional couplers. Left to right, a symmetric 180° bend coupler with a curvature radius of 20 mm, a symmetric 90° bend coupler with a curvature radius of 65 mm, and a nonsymmetric 180° bend coupler with a curvature radius of 20 mm.



(a)



(b)



(c)

Fig. 6. Theoretical and measured frequency characteristics of coupling  $|S_{31}|$  for: (a) a symmetric 180° bend coupler with a curvature radius of 20 mm, (b) a symmetric 90° bend coupler with a curvature radius of 65 mm, and (c) a nonsymmetric 180° bend coupler with a curvature radius of 20 mm. The effect of the field deformation at the bends is included in the solid curves, while it is ignored in the dotted curves.

calculated by neglecting it. More specifically, Fig. 6(a) illustrates the frequency dependence of the coupling for the symmetric coupler with a curvature radius of 20 mm. Measured values are in better agreement with the solid curves than with the dotted ones, demonstrating that the effect of the field deformation at a sharp bend cannot be ignored in the fabrication of couplers. Another important fact to be noted here is that complete power transfer can be expected if the coupling spacing is optimized. This is not the case in other dielectric waveguide couplers in which a linear section must be inserted between the two curved connecting arms to improve coupling [9], [10], [11]. The larger coupling coefficient of the NRD-guide is obviously the cause of this increase in coupling, as mentioned before.

Fig. 6(b) shows the results for another symmetric coupler consisting of 90° bends with a curvature radius of 65 mm. Since the bending radius is large, the effect of the field deformation is less important; hence the solid and dotted curves are not much different from each other. Fig. 6(a) and (b) together also supports the assertion that the theory holds regardless of bending angles of the component bends, since the coupling expressions are proved in the figures to equally apply to both the 180° and 90° bend couplers.

Fig. 6(c) shows the results for the nonsymmetric coupler. In this case, however, the measured values come closer to the dotted curves. This fact in no way implies that the field deformation at a bend is less important in nonsymmetric couplers. Instead, it should be considered that the modes in the straight and curved guides are not strictly degenerate; hence the difference in the propagation constants of the two guides results in a decrease in coupling. Nevertheless, the theory agrees well with measurements within practical accuracy and does not need any correction factor unlike the case of the dielectric waveguides of a rectangular cross section [11].

On the whole, the theoretical values deviate from measurements as the coupling spacing increases. The reason for this is that the field expression (5) is valid only in close proximity to the dielectric strip.

### B. 0-dB Coupler

Though a 0-dB coupler itself is not so important in practice as a 3-dB coupler, it can be a convenient standard estimating the coupling property of waveguides under consideration. On the basis of the present theory and using the three types of coupling structures described above, 0-dB couplers were designed and fabricated. Center frequencies for complete power transfer were set rather arbitrarily somewhere in the frequency range of 48 to 49 GHz because the coupling spacing could be adjusted only with a 0.1-mm step. The coupling spacings were found to be  $d_0 = 0.7$  mm for the symmetric coupler with a curvature radius of 20 mm,  $d_0 = 1.2$  mm for the symmetric coupler with a curvature radius of 65 mm, and  $d_0 = 1.0$  mm for the nonsymmetric coupler with a curvature radius of 20 mm.

Measured data for the scattering coefficients  $|S_{21}|$ ,  $|S_{31}|$ , and  $|S_{41}|$  are shown in Fig. 7(a), (b), and (c) as a function of frequency and compared with theoretical values which include the effect of the field deformation. Agreement

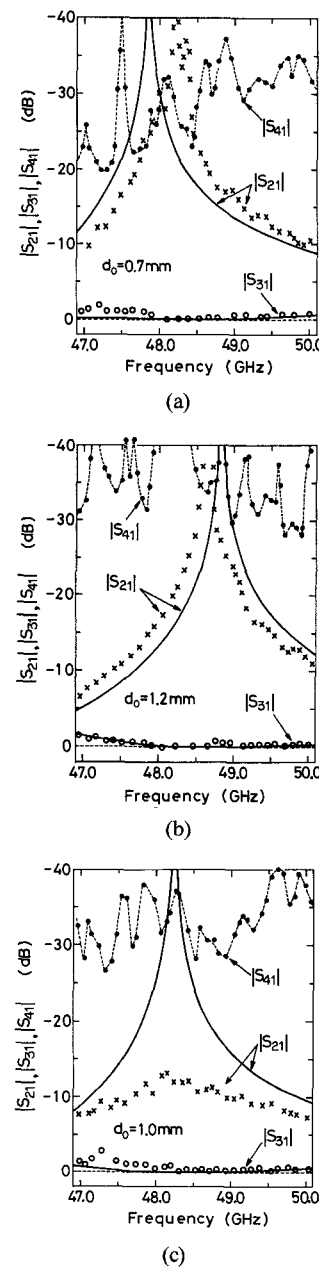


Fig. 7. Theoretical and measured frequency characteristics of 0-dB couplers consisting of: (a) coupled 180° bends with a curvature radius of 20 mm, (b) coupled 90° bends with a curvature radius of 65 mm, and (c) a straight guide coupled with a 180° bend having a curvature radius of 20 mm.

between theory and measurements is satisfactory and the complete power transfer can be observed in the predicted frequency range.

Values of  $|S_{21}|$  for both the symmetric couplers are as small as  $-40$  dB at the center frequencies. This is surprising considering the corresponding values of the image guide couplers,  $-15 \sim -25$  dB [10]. In the nonsymmetric coupler, however, it is about  $-13$  dB, being comparable with that of the nonsymmetric dielectric rod waveguide coupler [11]. The degradation in  $|S_{21}|$  value for the nonsymmetric coupler may be attributed to the difference in the propagation constants of the straight and curved guides, as pointed out before.

The worst value of  $|S_{41}|$  (directivity since  $|S_{31}| = 1$ ) was

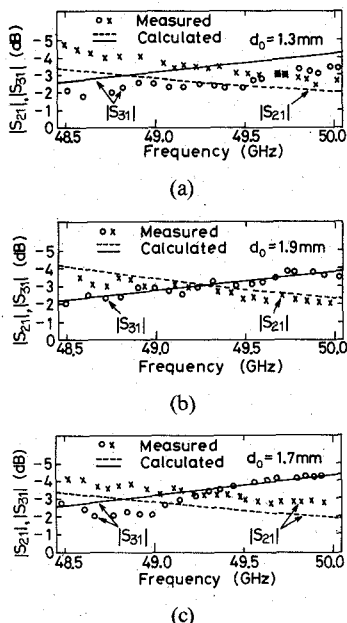


Fig. 8. Theoretical and measured frequency characteristics of quadrature hybrid couplers consisting of: (a) coupled  $180^\circ$  bends with a curvature radius of 20 mm, (b) coupled  $90^\circ$  bends with a curvature radius of 65 mm, and (c) a straight guide coupled with a  $180^\circ$  bend having a curvature radius of 20 mm.

found to be 20 dB for the symmetric coupler with a curvature radius of 20 mm. Since the coupling spacing is as small as 0.7 mm in this case, the perturbation due to the existence of the second guide would be so large to cause this degradation in directivity. If a straight section is inserted between the connecting arms, or if bends with a larger curvature radius are used, the directivity can be improved to some extent as is actually demonstrated in Fig. 7(b).

### C. Quadrature Hybrid Coupler

Quadrature hybrids are important in many applications including balanced mixer development [7]. The coupling spacings needed for half-power transfer are  $d_0 = 1.3$  mm and 1.9 mm for the symmetric couplers with curvature radii of 20 mm and 65 mm, respectively, and  $d_0 = 1.7$  mm for the nonsymmetric coupler with a curvature radius of 20 mm. Theoretical and measured data are shown in Fig. 8(a), (b), and (c). Agreement between them is satisfactory, and the well-balanced outputs are obtained over a frequency range of about 1 GHz. One possible disadvantage of the NRD-guide couplers may be their narrow bandwidth of operation, compared to other dielectric waveguide couplers [9]. Some ingenuity may be required to overcome this difficulty. The directivities ranged from 25 to 35 dB depending on the structure of each coupler, being better by about 5 dB than those of the 0-dB couplers because of larger coupling spacing.

### D. In-Phase Power Divider

The in-phase power divider was constructed in the configuration shown in Fig. 9 [8]. Power was fed to port 1 and extracted from ports 3 and 5. The curvature radius of the  $180^\circ$  bends was 20 mm. Since the effect of the nondegener-

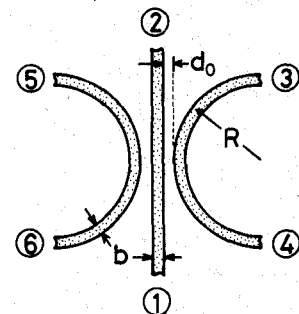


Fig. 9. Configuration of the in-phase power divider.

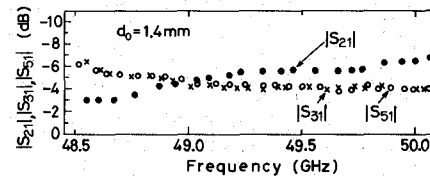


Fig. 10. Outputs of the power divider measured at coupled ports 3 and 5, and the rest detected at direct port 2.

ate modes is likely to be remarkable in this triple waveguide system, the theory could not predict the performance of the power divider very well. The construction had to be done experimentally and the best performance was achieved for the coupling spacing  $d_0 = 1.4$  mm. Measured data alone are shown in Fig. 10. The well-balanced outputs of 4 dB below the input could be obtained at ports 3 and 5 over a frequency range of about 1 GHz and the remaining power was detected at direct port 2.

### V. CONCLUSIONS

Characteristics of the curved NRD-guide directional couplers are analyzed by taking the effect of the field deformation at a bend into account. A simple theory is presented and confirmed experimentally to be useful for designing various couplers. Since the coupling coefficient of the NRD-guide is larger than those of other dielectric waveguides, 0-dB couplers, quadrature 3-dB hybrids, and a power divider could be fabricated by using polystyrene bends with a curvature radius as small as 20 mm at 50 GHz. In the nonsymmetric couplers and the power divider, the effect of the nondegenerate modes in the straight and curved guides is substantial and tends to decrease coupling. Although not examined in this paper, this effect must be included in the analysis to further improve the coupling theory.

### REFERENCES

- [1] T. Itoh, "Open guiding structures for millimeter-wave integrated circuits," *Microwave J.*, vol. 25, pp. 113-126, Sept. 1982.
- [2] T. Yoneyama and S. Nishida, "Nonradiative dielectric waveguide for millimeter-wave integrated circuits," *IEEE Trans. Microwave Theory Tech.*, vol. MTT-29, pp. 1188-1192, Nov. 1981.
- [3] T. Yoneyama and S. Nishida, "Nonradiative dielectric waveguide circuit components," in *Dig. 6th Int. Conf. Infrared Millimeter-Waves* (Miami), Dec. 1981.
- [4] T. Yoneyama, M. Yamaguchi, and S. Nishida, "Bends in nonradiative dielectric waveguides," *IEEE Trans. Microwave Theory Tech.*, vol. MTT-30, pp. 2146-2150, Dec. 1982.
- [5] K. Solbach, "The fabrication of dielectric image lines using casting resins and the properties of the lines in the millimeter-wave range,"

*IEEE Trans. Microwave Theory Tech.*, vol. MTT-24, pp. 879-881, Nov. 1976.

[6] T. Itanami and S. Shindo, "Channel dropping filter for millimeter-wave integrated circuits," *IEEE Trans. Microwave Theory Tech.*, vol. MTT-26, pp. 759-764, Oct. 1978.

[7] J. A. Paul and Y. Chang, "Millimeter-wave image-guide integrated passive devices," *IEEE Trans. Microwave Theory Tech.*, vol. MTT-26, pp. 751-754, Oct. 1978.

[8] J. A. Paul and P. C. Yen, "Millimeter-wave passive components and six-port network analyzer in dielectric waveguide," *IEEE Trans. Microwave Theory Tech.*, vol. MTT-29, pp. 948-953, Sept. 1981.

[9] R. Rudokas and T. Itoh, "Passive millimeter-wave IC components made of inverted strip dielectric waveguides," *IEEE Trans. Microwave Theory Tech.*, vol. MTT-24, pp. 978-981, Dec. 1976.

[10] K. Solbach, "The calculation and the measurement of the coupling properties of dielectric image lines of rectangular cross section," *IEEE Trans. Microwave Theory Tech.*, vol. MTT-27, pp. 54-58, Jan. 1979.

[11] T. Trinh and R. Mittra, "Coupling characteristics of planar dielectric waveguides of rectangular cross section," *IEEE Trans. Microwave Theory Tech.*, vol. MTT-29, pp. 875-880, Sept. 1981.

[12] D. Marcuse, "The coupling of degenerate modes in two parallel dielectric waveguides," *Bell Syst. Tech. J.*, vol. 50, pp. 1791-1816, July-Aug. 1971.

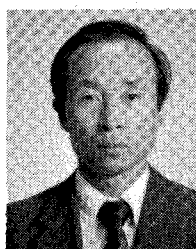
[13] T. Trinh and R. Mittra, "Field profile in a single-mode curved dielectric waveguide of rectangular cross section," *IEEE Trans. Microwave Theory Tech.*, vol. MTT-29, pp. 1315-1318, Dec. 1981.



**Norio Tozawa** graduated from Niigata University, Niigata, Japan, in 1981, and received the M.E. degree in electrical communication engineering from Tohoku University, Sendai, Japan, in 1983. He was mainly concerned with research into millimeter-wave integrated circuits there.

He is presently with Fujitsu Ltd., Kawasaki, Japan.

+



**Tsukasa Yoneyama** (S'60-M'69) graduated from Tohoku University, Sendai, Japan, in 1959, and received the M.E. and Ph.D. degrees in electrical communication engineering from the same university in 1961 and 1964, respectively.

He is currently an Associate Professor at the Research Institute of Electrical Communication, Tohoku University, where his research interests are concerned with electromagnetic field theory and millimeter-wave integrated circuits.

Dr. Yoneyama is a member of IECE of Japan.



**Shigeo Nishida** (SM'59) was born in Nagoya, Japan, on March 7, 1924. He graduated from Tohoku University, Sendai, Japan, in 1949, and received the Ph.D. degree from the same university in 1959.

He was appointed a Research Associate and an Associate Professor at the Research Institute of Electrical Communication, Tohoku University, in 1949 and 1955, respectively. From 1957 to 1959, on leave of absence from Tohoku University, he joined the Microwave Research Institute of the Polytechnic Institute of Brooklyn, Brooklyn, NY, where he was engaged in the research on microwave waveguides and antennas. Since 1964, he has been a Professor at Tohoku University, and his major interests are in microwave and optical-wave transmissions.

## A Compact Septum Polarizer

N. CHR. ALBERTSEN AND PER SKOV-MADSEN

**Abstract**—A waveguide polarizer with resonant notches in a septum is investigated. The Wiener-Hopf technique is employed to derive theoretical design data and the results are compared to experiments for a single-notch and a double-notch design. It is concluded that the agreement is good and the design useful for narrowband applications.

Manuscript received December 29, 1982; revised March 15, 1983. This work was sponsored by the Danish Space Board under Grant 1112-9/81.

N. Chr. Albertsen is with the Laboratory of Applied Mathematical Physics, Technical University of Denmark, Lyngby, Denmark.

P. Skov-Madsen is with the Electromagnetics Institute, Technical University of Denmark, Lyngby, Denmark.

### I. INTRODUCTION

IN ANTENNA systems where circular polarization is required, septum polarizers constitute a simple device for converting linear polarization into circular polarization in the feed waveguide. Examples of broad-band polarizer designs, based mainly on an experimental approach, are found in the literature, e.g., [1] and [2]. In the present paper, a narrow-band polarizer is analyzed analytically, using the Wiener-Hopf technique combined with Galerkin's method, and experimental test results for two specific designs are presented to validate the theoretical analysis.